

Non-linear mechanical response of the Red Blood Cell

Young-Zoon Yoon,^{1,2} Jurij Kotar,¹ Gilwon Yoon,² and Pietro Cicuti¹

¹*Cavendish Laboratory and Nanoscience Center, University of Cambridge, Cambridge CB3 0HE, U.K.*

²*Institute for Biomedical Electronics, Seoul National University of Technology, Seoul 139-743, Korea*

We measure the dynamical mechanical properties of human red blood cells. Single cell response is measured with optical tweezers. We investigate both the stress relaxation following a fast deformation, and the effect of varying the strain rate. We find a power law decay of the stress as a function of time, down to a plateau stress, and a power law increase of the cell's elasticity as a function of the strain rate. Interestingly, the exponents of these quantities violate the linear superposition principle, indicating a nonlinear response. We propose that this is due to breaking of a fraction of the crosslinks during the deformation process. The Soft Glassy Rheology Model accounts for the relation between the exponents we observe experimentally. This picture is consistent with recent models of bond remodeling in the red blood cell's molecular structure. Our results imply that the blood cell's mechanical behavior depends critically on the deformation process.

PACS numbers: 87.68.+z, 83.60.-a, 87.16.-b, 87.17.-d, 87.80.Cc

The human red blood cell is a biological structure of relative simplicity: it lacks a nucleus and intra membrane organelles. Its components are well characterized [1, 2, 3], and they can be summarized as a bilayer membrane, coupled to a thin tenuous cytoskeleton of spectrin filaments via two complexes of a few different proteins (ankyrin, band 3 and band 4.1). This outer membrane, held under tension by the cortical cytoskeleton, encloses a solution of dense haemoglobin. Despite its simplicity, the properties of this structure have puzzled researchers for decades. Investigations have focussed on two, related aspects: explaining the biconcave discocyte shape that is found under physiological conditions (and a whole array of other morphologies that are found under perturbation or disease); measuring the mechanical properties of the structure. Regarding the shape, significant progress has been made recently showing how, by carefully balancing the membrane bending elasticity with a tension from the underlying spectrin scaffold, the discocyte shape emerges as the equilibrium solution, and the cup-shaped stomatocyte is the result of a perturbation that decreases the membrane area relative to the underlying skeleton [3]. On the issue of mechanics and dynamics of the structure, our understanding is still very limited, despite the great importance of these parameters. Large deformations of the cell are involved in blood flow through thin capillaries, and the cells in suspension more generally determine the peripheral blood rheology in healthy and diseased conditions [4]. The red blood cell has variously been described as either liquid or solid [5].

In this Letter we investigate the dynamical mechanical properties of the red blood cell by measuring its viscoelasticity over a range of environmental conditions. We focus on the effect of the cell age, of the deformation dynamics, and the correlation between the cell modulus and its shape. We relate the findings to phenomenological models for flow in kinetically arrested systems, and to recent models describing the metabolic activity of the RBC, where the consumption of ATP controls the stiffness of the elastic network [6, 7, 8]. The nor-

mal biconcave human RBC has approximately 25% more membrane surface area than the minimum required to enclose its volume, allowing deformations without extension of the membrane [9]. Therefore the mechanical response of the cell is related only to its bending and shear elastic moduli, and its membrane and bulk viscosities. These quantities have been measured with various techniques, in particular micropipette aspiration, shape flickering, deformation in flow, and optical tweezers. Existing measurements give very different values. For example, independent experiments using micropipette aspiration yield a shear modulus of between 6 and 10 $\mu\text{N/m}$ [10]. Optical tweezers measurements report a wide range of shear modulus, but the discrepancies between these results are in part the result of applying different geometrical models to extract the modulus from the measured forces: $2.5 \pm 0.4 \mu\text{N/m}$ assuming a flat disk geometry [11]; 200 $\mu\text{N/m}$ assuming a spherical initial shape [12, 13]; 11 to 18 $\mu\text{N/m}$ comparing to a finite element simulation of the deformation [14]. A satisfactory approximation for the deformation geometry is still not available, and is not the topic of this Letter. We choose instead to report the directly measured mechanical properties, showing that even the model-independent dynamical stiffness of the cell is strongly dependent on the deformation protocol. Our key result is that the RBCs response cannot be explained within the framework of linear viscoelasticity.

Fresh blood was drawn from a healthy volunteer donor, and diluted in phosphate-buffered saline (PBS) with acid citrate dextrose (Sigma C3821) and 1mg/ml bovine serum albumin (BSA) (Sigma A4503) at pH7.4. For studying the effect of aging time after drawing, cells were incubated with glucose-free PBS either in a hot bath plate at 37°C for 24h with 10^{-2} Penicillin-Streptomycin solution (GIBCO, Invitrogen 15070063) to prevent microbial growth, or at 4°C for 24h. A first control group was formed by adding 1mM MgATP (Sigma A9189), after the 24h incubation, to the the RBCs in glucose-free PBS suspension. A second control group was incubated with 100mg/dl glucose in PBS buffer. These protocols provide

samples that are a mixture of discocyte and stomatocyte cells, with an increasing fraction of discocytes after 1 day's incubation.

The optical tweezers setup consists of a laser (IPG Photonics, PYL-1-1064-LP, $\lambda=1064\text{nm}$, $P_{max}=1.1\text{W}$) focused through a water immersion objective (Zeiss, Achromplan IR 63x/0.90 W) trapping from below. The laser beam is steered via a pair of acousto-optic deflectors (AA Opto-Electronic, AA.DTS.XY-250@1064nm) controlled by custom built electronics allowing multiple trap generation with sub nanometer position resolution. The trapping potential is locally described by a harmonic spring, and the trap stiffness was calibrated by measuring the thermal displacements of a trapped bead. The trapping stiffness at maximum power when trapping two beads (as in this work) is $k_{trap}=44\text{pN}/\mu\text{m}$ on each bead. The sample is illuminated with a halogen lamp and is observed in bright field with a fast CMOS camera (Allied Vision Technologies, Marlin F-131B).

Carboxylated silica beads of $5.0\mu\text{m}$ diameter (Bangs Labs) were washed in Mes buffer (Sigma M1317). They were then functionalized by resuspending in Mes buffer and incubating for 8h at 37°C with Lectin (0.25mg/ml) (Sigma L9640) and EDC (Sigma E1769) (4mg/ml). This made them very sticky to the RBC, probably through binding to glycoproteins or sugars on the outer side of the RBC membrane. To prevent the RBCs from sticking on the glass surfaces of the chamber, BSA was coated on the slide glass. Using the tweezers, two beads are brought to an RBC and attached diametrically across a cell, which is then floated well above the glass slide surface (at about 10 times the bead diameter) to minimize any hydrodynamic drag from the solid surface. The cells are quite monodisperse in size, with an initial cell length (the diameter) $L_0 \sim 8\mu\text{m}$. The area of contact between the bead and the cell varies in the range $3\text{--}4.5\mu\text{m}^2$, and we find no correlation of the patch area with any of the experimental results. This arrangement is drawn in Fig-

ure 1. During all the deformation protocols, one laser trap is kept fixed at its initial position, while the other trap is moved away by a distance Δlaser . We focus on tracking the bead in the immobile trap, measuring the difference Δx between the bead and the known laser position using image analysis code written in Matlab. From the displacement Δx , the stretching force is calculated. The cell is elongated by a distance $\Delta L = \Delta\text{laser} - 2\Delta x$, and we define the strain as $\gamma = \Delta L/L_0$. The resolution of bead position via image analysis on each frame is around 5nm , which translates into $\pm 0.22\text{pN}$ of force resolution. This is significantly less than the random fluctuations caused by thermal noise. The cell stretching is recorded at ~ 60 frames per second, and having checked that we could not observe a variation between measurements done at room temperature and at 37°C , we report on measurements made at room temperature. Temperature is known from previous studies to have only a slight influence on the mechanics of red blood cells [15, 16].

We perform stress relaxation experiments by moving just one trap (i.e. moving one bead) by $\Delta\text{laser}=3.5\mu\text{m}$ at $20\mu\text{m/s}$, and monitoring the force acting on the stationary bead. The force is observed to decay towards a plateau value, which is reached within less than half a minute. We define the time-dependent stiffness of the red blood cell to be $\kappa(t) = F(t)/\Delta L(t)$. The whole set of experiments is fit very well by the 3-parameter power law function:

$$\kappa(t) = \kappa_\infty + \Delta\kappa(t) = \kappa_\infty + \Delta\kappa_0 (t/t_0)^{-\alpha}, \quad (1)$$

where we fix $t_0 = 1\text{s}$ to obtain a dimensionless time. We use the first 20 seconds of the decay to fit these values, where there is less noise in the data, but it can be seen that the power law decay holds for longer times as well. In contrast, a single exponential fails to fit the data and even a stretched exponential (4-parameters) gives a poor fit. Figure 1 shows examples of the time relaxation of $\Delta\kappa(t)$ plotted separately for each of discocyte and cup shaped stomatocyte cells, fresh and after one day of incubation. In all cases the stiffness is fit over two decades in time by the form of Eq. 1. The power law exponents are the same within experimental error, the mean of all the power law exponents measured is $\alpha=0.75\pm 0.16$ for fresh cells and $\alpha=0.82\pm 0.09$ for 1-day old cells. A total of 11 different cells were measured this way. The value of the ratio $\Delta F_0/F_\infty$, i.e. the fraction of the stress that decays over time, also appears independent of shape and cell age, and is between 0.55 and 0.75. The fact that the data is described so well by Eq. 1 implies that there are two components to the cell elastic modulus: a time-dependent and a long-time equilibrium modulus. Power-law relaxations are well known in systems near the gelation point and in entangled polymer solutions [17], however we anticipate here that we will discuss how for the red blood cell the form of Eq. 1 does not originate from polymer relaxation nor gel cluster dynamics. To investigate further the strain rate dependence of the cell modulus, we perform a triangle wave deformation exper-

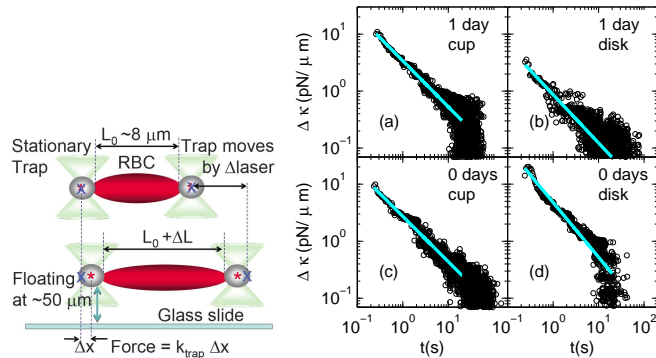


FIG. 1: Diagram of experimental setup. A cross marks the positions of the laser trap and a star marks the center of the bead, obtained via image analysis. (a)-(d) Decays of the measured time-dependent cell stiffness $\kappa(t)$ as a function of time. The plateau value has been subtracted. This data shows a power law decay with exponents $\simeq 3/4$.

iment using speeds of 20, 5, 1 and $0.2\mu\text{m/s}$, and $3.5\mu\text{m}$ laser trap displacement [25]. Figure 2(a) shows that the force measured over time is approximately proportional to the applied strain. The slight mismatch between the applied strain and the stress can be seen more clearly in Figure 2(b) as a hysteresis loop. There is a slight difference between the onset of the first cycle and all the following ones: From observing many instances of this protocol we believe that this is due to the cell rearranging its position precisely along the axis of the strain experiment. It is clear from this figure that there is no further evolution of the stress strain curves over the run, which lasts typically tens of cycles. The cell's response is predominantly elastic, and the gradient of the force vs. elongation data as in Figure 2(b), taken over the extension, gives the stiffness κ of the cell. This stiffness is an effective property of the cell, a valid modulus for describing the cell's response in physiological processes such as squeezing through thin capillaries. Our results show that there can be a large (factor of three) difference between the dynamic and static stiffness, as measured for example by micropipette. The experimental speed of deformation can be converted into an approximate strain rate $\dot{\gamma}$ by dividing the bead velocity by the initial cell length (L_0). The cell stiffness is plotted in Figure 3 against the strain rate. These quantities are seen to be approximately related through the function:

$$\kappa(\dot{\gamma}) - \kappa_0 \sim \dot{\gamma}^\beta, \quad (2)$$

with $\beta \simeq \frac{1}{4}$.

The hysteresis in the stress strain curves is a measure of energy dissipation in the cell, and is shown in Figure 3. In order to compare results from different strain amplitudes, the dissipated energy is presented as the work per cycle, normalized by the square of the strain amplitude γ_{max} . The dissipated energy follows a power law as a function of strain rate, with an exponent that we assume is the same β as in Eq. 2. In all the cells the strain rate dependence is well below the linear relation expected for a purely viscous system. The exponents fitted here are $\beta = 0.25$ for fresh discocytes and $\beta = 0.33$ for discocytes

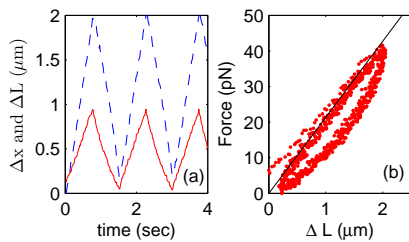


FIG. 2: (a) The dashed line is the elongation ΔL of the red blood cell subject to a triangle wave trap displacement, and the solid line is Δx of the bead in the stationary trap. (b) Force vs. elongation of the cell ΔL , for the same data as in panel (a). Solid line is a linear fit to the force during extension, the area inside the hysteresis loop is the energy dissipated per cycle.

after one day's incubation. These values have a higher precision than the stress relaxation exponents because the triangle wave cycle is repeated many times. [26] In linear viscoelasticity, the dependence of the modulus on the strain rate is related to the form of the stress relaxation via a modified Laplace transform [17]. In the case of a power law decay with $\kappa(t) - \kappa_\infty \sim t^{-\alpha}$, we expect $\kappa(\dot{\gamma}) - \kappa_0 \sim \dot{\gamma}^\alpha$. This is very clearly not the case here, the exponent β is much smaller than α . This points to the fact that even though our strain amplitudes are not very large, only of the order of 20%, our experiment is in a nonlinear regime. This finding can be understood as follows: the power law relaxation is the manifestation of a system where at least a fraction of the bonds can break under stress and quickly reform, essentially remodeling the skeleton's network. There is an analogy between this molecular-scale picture and the more general situation of the rheology of a system where the components have to overcome potential barriers in order to flow. This condition is addressed by the soft glassy rheology (SGR) model which, assuming a distribution of energy wells of different depths, provides a framework for calculating the nonlinear response of the system [18]. It contains one principal parameter, x , which is the ratio between the available energy and the mean well depth. For $x < 1$ the model is in a glassy phase. The shear modulus is predicted to decay with time as $G \sim t^{-x}$, and the stress under constant strain rate is $\sigma - \sigma_y \sim \dot{\gamma}^{1-x}$. The red blood cell power laws and exponents appears to be well described by the SGR model with a value of $x \simeq 3/4$. In the red blood cell it is likely that the potential barriers to be overcome are the energies for releasing a spectrin filament from a crosslink. The filament would then re-bond in a configuration of lower stress. The presence of a long lived residual stress in the stress relaxation implies either the presence of a fraction of permanent bonds, or of a kinetically arrested state with residual stress, leading to a deviation from a purely power law scaling at low strain rates which is visible in the stiffness data of Figure 3.

In the absence of external stresses it is known that ATP is required to open the spectrin-actin linker, whose bond energy is around $7k_B T$, i.e. $3 \times 10^{-20} \text{J}$ [19, 20]. Based on the known mesh size of the cytoskeleton (between 80-100nm) and the cell surface area, we can estimate the order of magnitude of the number of bonds to be 10^4 . Given that the dissipated energy per cycle is of the order of 10^{-17}J this implies that either only a small fraction of the bonds, around 3%, is broken during a cycle, or that the bond energies under stress are reduced considerably, or that ATP and not solely mechanical energy is being used to break the bonds. Of these possibilities the agreement with the soft glassy rheology observed here suggests that remodeling of the linkers under stress does not involve the full cost of breaking the spectrin-actin linker. While the features of the dynamical response of all the cells are the same, we observe differences in the magnitude of the response depending on the shape of cell and the incubation protocol. The strongest influence, lead-

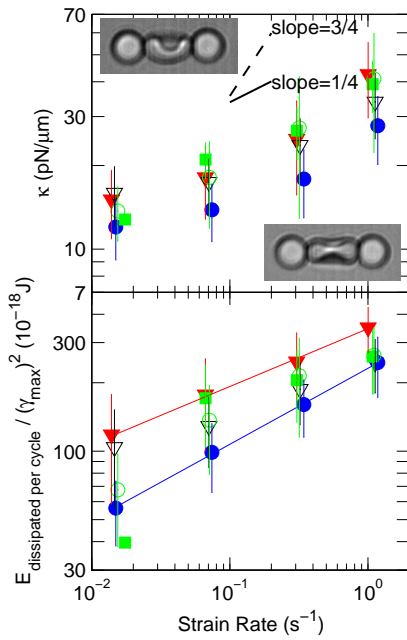


FIG. 3: Strain rate dependence of the RBC stiffness κ and the energy dissipation. Markers indicate the different conditions studied here: (\blacktriangledown) fresh-Discotic; (∇) fresh-Stomatocyte; (\bullet) 1day-Discotic; (\circ) 1day-Stomatocyte; (\blacksquare) 1day-discotic +MgATP.

ing to a decrease of the cell modulus of almost a factor of 2 after 1 day of incubation, is the time from when the cells are drawn. Secondary to this aging, we observe a correlation between the stiffness of the cell and its shape. The cup-shaped stomatocytes are almost twice as stiff as the discotic cells. Models proposed recently describe the active remodelling of the RBC's cytoskeletal network [8, 20]. ATP is expected to be strongly related to this activity, at least under absence of an external force [8]. It is of interest that flickering of the membrane at low frequencies was shown to depend on the intracel-

lular MgATP[21], and the flickering has also been shown to decrease with cell aging [15]. Through the 1-day incubation protocol the ATP concentration inside the cell is depleted, and according to these references this would lead to stiffer cells. Our results showing softening seem to imply an opposite effect, one possibility is that under reduction of ATP the cell loses some of its ability to reform the bonds that break under deformation. We find no appreciable difference between aging in the absence of glucose and in physiological glucose concentrations (data not shown). We find a strong effect adding MgATP to an aged cell: MgATP causes an increase of both the stiffness and dissipation for the discotic cells, bringing the values close to those of freshly drawn cells.

The rate dependence of the cell modulus measured in this work can be also be compared to recent data obtained by monitoring the deformation induced via magnetic twisting cytometry (MTC). This is essentially a creep experiment performed on a pivoting magnetic bead bound to the outside of a red blood cell [22]. In MTC there is almost certainly a large influence of the membrane bending elasticity, and the data in ref. [22] is dominated by a source of elasticity that is not found in our measurements with optical tweezers. Our data confirms that the dynamics in the red blood cell, as also pointed out by Suresh and collaborators, is intrinsically free of a characteristic timescale [22]. In addition we have shown here that the dynamics is not linear, and therefore depends on the deformation protocol, even for small deformations. This may be relevant to other cell types. Our findings here are in contrast to many previous investigations of the red blood cell [11, 14, 23], where limited datasets led to simplistic conclusions regarding the dynamics.

We acknowledge funding by the Oppenheimer Fund, EPSRC, and the Cavendish-KAIST programme of MoST Korea. We thank I. Poberaj, N. Gov, E.M. Terentjev, J. Guck, J. Sleep, J. Evans, W. Gratzner and P.G. Petrov for advice and help.

-
- [1] B. Alberts, D. Bray, J. Lewis, M. Raff, K. Roberts, and J. D. Watson, *Molecular Biology of the Cell* (Garland Publishing, New York, 1994).
 - [2] D. Boal, *Mechanics of the cell* (Cambridge University Press, U.K., 2002).
 - [3] G. H. W. Lim, M. Wortis, and Mukhopadhyay, PNAS **99**, 16766 (2002).
 - [4] S. Suresh, J. Mater. Res. **21**, 1871 (2006).
 - [5] R. M. Hochmuth, Ann. Rev. of Biophys. and Bioeng. **11**, 43 (1982).
 - [6] S. Tuvia, S. V. Levin, and R. Korenstein, Biophys. J. **63**, 599 (1992).
 - [7] S. Tuvia, S. Levin, A. Bitler, and R. Korenstein, Biophys J. **141**, 1151 (1999).
 - [8] N. S. Gov, Phys. Rev. E **75**, 011921 (2007).
 - [9] A. W. L. Jay, Biophys. J. **15**, 205 (1975).
 - [10] R. Waugh and E. A. Evans, Microvasc. Res. **12**, 291 (1976).
 - [11] S. Hénon, G. Lenormand, A. Richert, and F. Gallet, Biophys J. **76**, 1145 (1999).
 - [12] J. Sleep, D. Wilson, R. Simmons, and W. Gratzner, Biophys J. **77**, 3085 (1999).
 - [13] K. H. Parker and C. Winlove, Biophys J. **77**, 3096 (1999).
 - [14] M. Dao, C. T. Lim, and S. Suresh, J. Mech. Phys. Solids **51**, 2259 (2003).
 - [15] K. Fricke and E. Sackmann, Biochim. Biophys. Acta **803**, 145 (1984).
 - [16] G. M. Artmann, Biorheology **32**, 553 (1995).
 - [17] R. G. Larson, *The Structure and Rheology of Complex Fluids* (Oxford Univ. Press, New York, 1999).
 - [18] P. Sollich, F. Lequeux, P. Hébraud, and M. E. Cates, Phys. Rev. Lett. **78**, 2020 (1997).

- [19] V. Bennett, *Biochim. Biophys. Acta* **988**, 107 (1989).
- [20] N. S. Gov and S. A. Safran, *Biophys. J.* **88**, 1859 (2005).
- [21] S. V. Levin and R. Korenstein, *Biophys. J.* **60**, 733 (1991).
- [22] M. Puig-de Morales-Marinkovic, K. T. Turner, J. P. Butler, J. J. Fredberg, and S. Suresh, *Am. J. Cell Physiol.* **293**, 597 (2007).
- [23] R. M. Hochmuth, P. R. Worthy, and E. A. Evans, *Biophys. J.* **26**, 101 (1979).
- [24] P. Cicuta, S. L. Keller, and S. L. Veatch, *J. Phys. Chem. B* **111**, 3328 (2007).
- [25] For one speed and condition (data not shown) we applied a triangle wave of amplitudes 1, 5 and 7 μm and obtained the same stiffness as for 3.5 μm .
- [26] We consider here how much dissipation can arise from the phospholipid bilayer itself. Its viscosity is around 0.3Pa s, ref. [24]. For a simplified geometry of deformation of two flat plates, the dissipated energy is around $0.6 \times 10^{-18} \text{J}$ per cycle at $\dot{\gamma} = 10^{-2} \text{s}^{-1}$. This is an order of magnitude below our results but, growing linearly with strain rate, it would dominate the response at higher deformation rates.